

NANO-GRAINED STEELS PRODUCED BY VARIOUS SEVERE PLASTIC DEFORMATION PROCESSES

M.Umemoto*, Y.Todaka and K.Tsuchiya

Department of Production Systems Engineering, Toyohashi University of Technology, Toyohashi, Aichi 441-8580

Abstract

The formation of nanocrystalline structure (NS) in steels by various severe plastic deformation processes, such as ball milling, a ball drop test, particle impact deformation, drilling, sliding wear, ultrasonic shot peening and air blast shot peening was studied. Nanograined regions were produced near the specimen surface. The deformation induced nanograined regions have the following common specific characteristics: 1) with grains smaller than 100 nm, 2) extremely high hardness, 3) dissolution of cementite when it exist and 4) no recrystallization and slow grain growth by annealing. It was suggested that the most important condition is to impose a strain larger than about 7.

Keywords: nanocrystal, severe plastic deformation, steels, shot peening

Introduction

Large efforts have been devoted to refine grains of materials since ultrafine-grained materials have often superior mechanical and physical properties to those of coarse-grained counterparts. Among the various methods proposed to obtain nanograined materials (grain size smaller than 100 nm) [1,2], severe plastic deformation [3,4] has received the largest attention due to the simplicity and applicability for all class of materials. Figure 1 shows representative severe plastic deformation processes to produce nanocrystalline structure (NS):

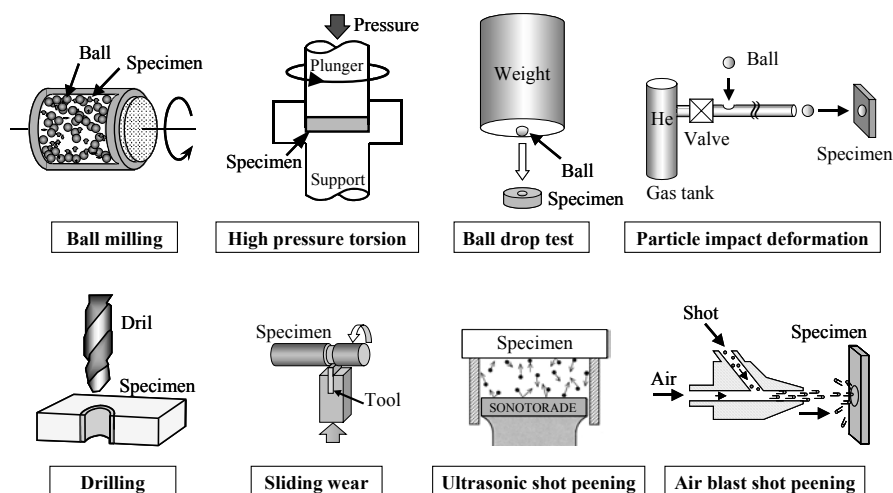


Fig.1 Various severe plastic deformation processes to produce nanocrystalline structure

* Corresponding Author. umemoto@martens.tutse.tut.ac.jp

ball milling [5,6], high pressure torsion [7], a ball drop test [8], particle impact deformation [9], drilling, sliding wear [10], ultrasonic shot peening [11] and air blast shot peening [9,12]. In the present study the microstructure evolutions in steels by these methods (except high pressure torsion) were observed. Focusing on iron and steels, the amount of strain, strain rate to produce NS are discussed.

Experimental Procedures

The materials used in the present study were Fe-0.10C (Fe-0.099C-0.20C-1.37Mn in mass% hereafter, martensite structure), Fe-0.15C (Fe-0.15C-0.35Si-1.24Mn, ferrite+cementite), Fe-0.80C (Fe-0.800C-0.20Si-1.33Mn, pearlite or spheroidite structure), Fe-3.3Si (Fe-0.027C-3.29Si-0.01Mn, ferrite) and the case hardening SCM420H steel. The details of the experimental conditions of ball milling, a ball drop test, particle impact test and air blast shot peening (ABSP) were described in our previous papers[8,9,13]. The drilling test was performed using a drill of 2.5 mm in diameter with cutting speed of 50 m/min and feed of 0.05 mm/rev. Oil mist was used for coolant. Wear test was performed using a rod sample (15 mm in diameter) and a plate tool (5 mm wide). The tool was made of SKD61 (alloy tool steel for hot dies and hardness of HV 850). A rod specimen was rotated with a speed of 25 rpm (sliding speed of 1 m/s) and rubbed by the tool for 5 mm as is shown in Fig.1. Running methanol (50 cc/min) was used for a coolant. Ultrasonic shot peening (USSP) was performed for 1.8 ks using JIS SUJ2 shot (0.4 mm in diameter). In the experiment, the shots were placed in the chamber vibrated (frequency: 20 kHz, amplitude: 90 μ m) by a generator, with which the shots were resonated as is shown in Fig.1. The projection distance was 10 mm. Annealing of nanocrystallized specimens was carried out at 873 K for 3.6 ks by sealing in a quartz tube under a pure Ar protective atmosphere. Specimens were characterized by SEM, TEM and Vickers microhardness tester (load of 0.25 N for 15 s). Specimens for SEM observations were etched by 5 % Nital.

Results

Nanocrystallization by Ball Milling

Figure 2 shows SEM micrographs of the ball milled Fe-0.1C martensite with initial hardness of 3.2 GPa. From the full view of the cross section of a powder (Fig. 2 (a)) two distinct regions are recognized. One is the dark uniform contrast region with several tens of μ m thick observed near the surface of powder and the another is the bright contrast region observed interior of the powder with deformed martensite morphology. The hardness of dark contrast region (8.8 GPa) is much higher than that of bright contrast region (3.9 GPa) as shown in Fig. 2 (b). The boundaries between these two types of regions are clear and sharp. There is no intermediate structure between these two regions. TEM observation (shown below) revealed that the dark contrast area corresponds to nanograin structured region and the bright contrast area corresponds to dislocated cell structured region, respectively. These two types of structures were observed in all the ball milled carbon steels irrespective of the carbon content (0 ~ 0.9 mass%C) or starting microstructure (ferrite, martensite, pearlite or spheroidite).

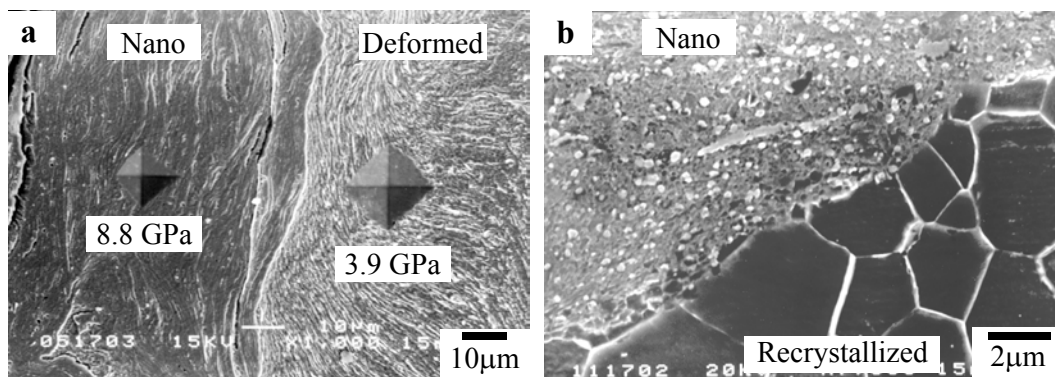


Fig.2 SEM micrographs of Fe-0.10C martensite ball milled for 360 ks. (a) as ball milled and (b) after annealed at 873 K for 3.6 ks.

Nanocrystallization by a Ball Drop Test and particle impact deformation

NS can be produced near the surface of specimens after one or several times of a ball (weight attached) drops. Figure 3 shows a typical dark contrast layer formed in Fe-0.15C with fine grained ferrite structure (Fig.3(a)) and in Fe-0.80C specimen with pearlite structure (Fig.3(b)), respectively. The microhardness of the dark contrast layer is much higher than the adjacent region with deformed structure.

Figure 4 shows a typical nanocrystalline layers formed in pearlitic Fe-0.80C specimen after particle impacts at LN₂ temperature. The dark contrast layer of about 10 μm thickness observed on the top surface was confirmed as nanocrystalline region by TEM observation. The microhardness of the nanocrystalline region (9.7 GPa) is substantially higher than the subsurface region with deformed structure (4.5 GPa).

Nanocrystallization by drilling and wear

The microstructure along the depth from the surface of drill hole is shown in Fig.5. In the picture the hole is at the top and drilling direction is located horizontally. The specimen used was a case hardening steel (SCM420H). The specimen was carburized and quenched to obtain martensite structure. Uniform contrast layer is seen near the surface. TEM observation revealed that the microstructure close to the surface is equiaxed grains with about 100 nm in diameter. It is considered that the drill hole surface received a strain heavy enough to produce nanocrystalline structure. The microhardness of the nanocrystalline region (7.3 GPa) is much higher than the subsurface region with deformed martensite structure (4.0 GPa).

NS can also be produced by wear test. In the present study SKD61 tool was slid against the rod of Fe-0.10C specimen with martensite structure. After sliding wear test, homogeneous contrast layer was observed at the surface of specimen. Figure 6 shows wear tested specimen

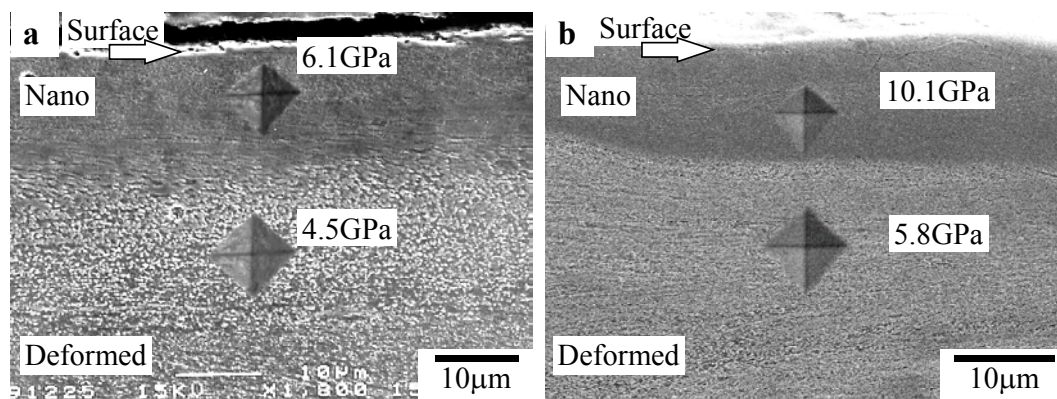


Fig. 3 SEM micrographs after a ball drop test. (a) Fe-0.15C fine grained ferrite and (b) Fe-0.80C pearlite.

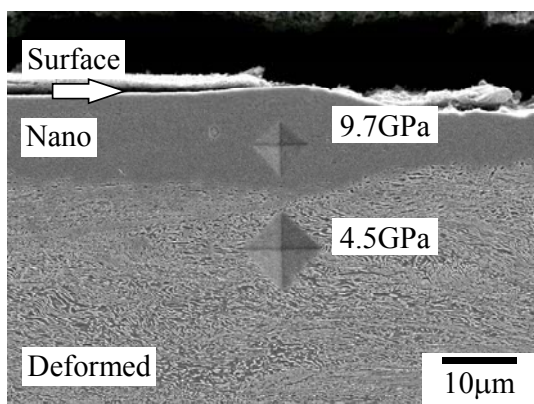


Fig. 4 SEM micrograph after particle impact deformation. Fe-0.80C pearlite impacted 8 times at LN₂ temperature.

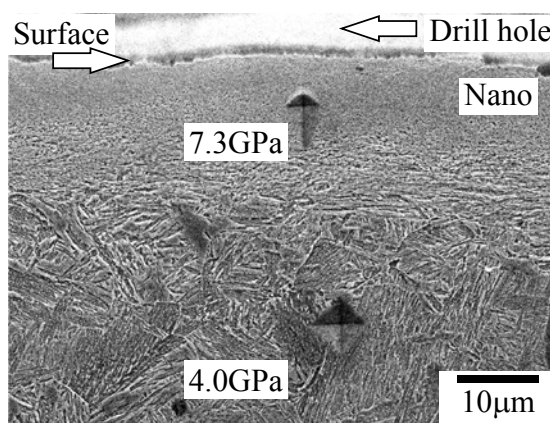


Fig. 5 SEM micrograph after drilling of carburized SCM420H.

after annealing. It is seen that homogeneous structure region at the top surface remains unchanged in contrast to the underneath recrystallized region in which clear grain boundaries are seen. From the unique structure, annealing behavior and microhardness, it is concluded that NS was produced by the present wear test.

Nanocrystallization by Shot Peening

Figure 7 shows SEM micrograph of Fe-3.3Si specimen after USSP and subsequent annealing. The top surface layer of several μm thick shows homogeneous structure without grain boundaries. This suggests that NS was produced by USSP as previously reported[11]. Underneath this NS layer is conventional work-hardened region which turned out to be conventional recrystallized morphology after annealing. It was noted that the thickness of the nanocrystalline layer produced by USSP is much thinner than that of conventional air blast shot peening. This is mainly due to difference in shot speed (20 m/s in USSP and 120m/s in ABSP). It should be noted the boundary between the NS and recrystallized (originally deformed structure) region is clear similar to those observed in various severe plastic deformation processes shown here.

Figure 8 [13] shows cross section of near surface area of ABSP treated Fe-0.8C specimen (spheroidite structure pre-strained 84 % by cold rolling) after shot peening (a) and after shot peening and annealing (b). Nanocrystalline layer with 5 μm thickness is produced at the top surface. Before ABSP, the spherical cementite particles with diameter about 0.5 μm were uniformly distributed in the ferrite matrix. After ABSP, cementite particles are not visible in the nanocrystalline surface layer. This indicating that the dissolution of cementite takes place in the nanocrystalline layer similar to other severe plastic deformation processes mentioned above. After annealed at 873 K for 3.6 ks, nanograined region did not show any detectable change while the deformed structured regions below the nanograined region showed recrystallized structure.

The production of nanocrystalline surface layer by ABSP has considerable industrial

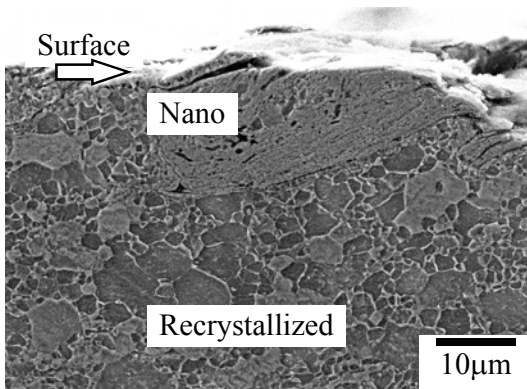


Fig. 6 SEM micrograph of wear tested Fe-0.10C martensite.

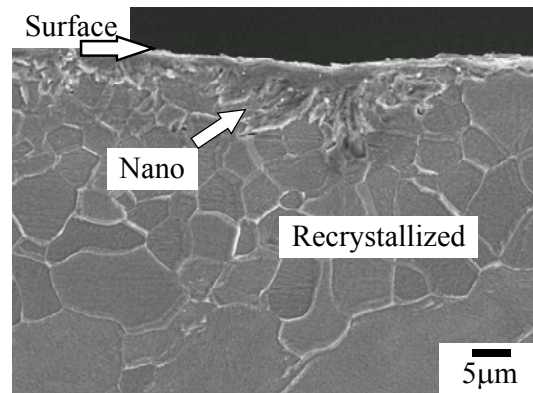


Fig. 7 SEM micrograph of ultra sonic shot peened Fe-3.3Si. Specimen was annealed after peening.

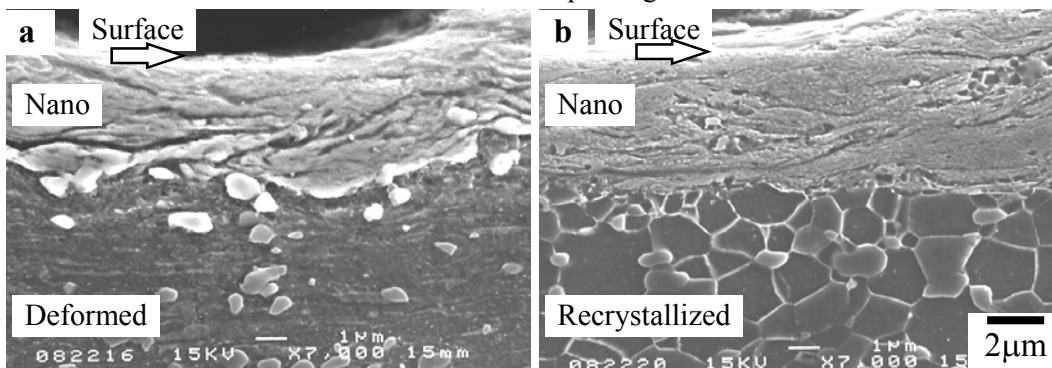


Fig. 8 SEM micrographs of Fe-0.80%C steel with spheroidite structure (84 % cold rolled before shot peening) after shot peening (< 50 μm in shot diameter, 190 m/s in shot speed, 10 s in peening time and 1000 % in coverage). (a) as shot peened and (b) after annealing at 873 K for 3.6 ks.

importance since ABSP is a popular process in industries and it can produce nanostructured surface layer with a high productivity. Industrial application of this new technology is expected especially to upgrade the traditional engineering materials.

Discussion

Impose a large strain seem to be the most important condition to produce nanocrystalline structure (NS). The reported amount of strain applied to obtain NS (grain size less than 100 nm) varies from 7 to 31 depending on the deformation techniques and materials employed.

The amount of strain can be measured well in drawing and torsion experiments. Langford and Cohen [14]) studied the drawn Fe up to $\epsilon = 6$ and reported that the flow stress increased linearly with strain up to 1.4 GPa. Extrapolating their flow stress vs strain data, the strain which gives the flow stress corresponding to $d = 100$ nm (2.1 GPa estimated from the Hall-Petch relationship for iron[13]) (*i.e.*, σ [GPa] = $0.12 + 20d^{-1/2}$, d in nm)) is expected to be attained at $\epsilon = 12$. Tashiro[15]) reported the flow stress of drawn iron wire strained up to $\epsilon = 11.5$. The flow stress corresponding to $d = 100$ nm (2.1 GPa) is achieved at $\epsilon = 7$. The experiment of high pressure torsion straining in iron was carried out by Valiev *et al* [16]). After 3 turns ($\epsilon = 108$) the hardness reaches 4.5 GPa and tends to reach a steady state. The grain size about 100 nm was obtained after 5 turns ($\epsilon = 180$) at which the hardness was 4.6 GPa. Similar torsion experiment has been done by Kaibyshev *et al* [17]) in Fe-3%Si. After straining to $\epsilon = 31$ (0.5 turn), grains are reduced to 120-200 nm and the microhardness increased to 7.2 GPa. From the obtained microhardness it can be considered that the grain size less than 100 nm was achieved. From the hardness measurement $d = 100$ nm (6.3 GPa) is expected to be accomplished at a strain $4.3 < \epsilon < 31$.

The amount of strain to produce NS was also estimated in a ball drop test and sliding wear test, although with less accuracy. In a ball drop test, Umemoto *et al* [18]) estimated $\epsilon = 7.3$ at strain rate of around 1.3×10^4 /s. Hughes and Hansen[19]) studied the nanostructures in Cu produced by sliding. The amount of strain to reach $d = 100$ nm is estimated to be 8. Summarizing the above mentioned studies, the minimum amount of strain necessary to produce NS is considered to be around 7-8, although it depends on materials, microstructure, deformation techniques and deformation conditions employed.

Figure 9 demonstrates the amount of strain and strain rate range of various deformation processes. In the figure, the range in which nanocrystallization is observed are shown. It is expected that nanocrystallization occurs when the amount of strain becomes larger than about 7 irrespective of the strain rate or kind of deformation processes employed. High strain rate deformation may not be a necessary condition to produce NS but it probably enhance local strain concentration due to plastic instability induced by deformation heat.

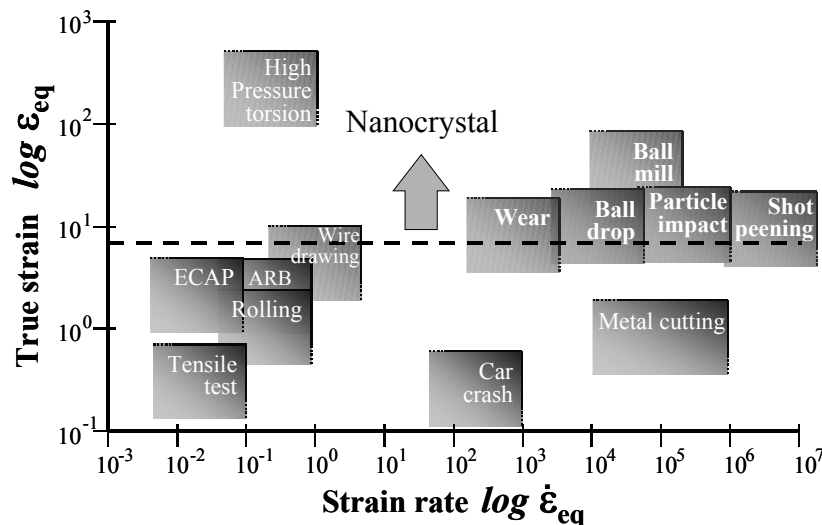


Fig. 9 The range in the amount of strain and strain rate to produce nanocrystalline structure in steels. The range of each deformation processes is shown.

Summary and conclusions

(1) Nanocrystalline structures can be produced in steels by ball milling, a ball drop test, particle impact deformation, drilling, sliding wear, ultra sonic shot peening and air blast shot peening. The hardness of nanograined region is extremely high. The cementite dissolves completely when the nanocrystallization of ferrite matrix starts.

(2) By annealing, nanograined region showed substantially slow grain growth without recrystallization.

(3) To produce nanograined structure by deformation, a large strain (larger than about 7) is probably the most important condition.

Acknowledgements

This work is partly supported by the Grant-in-Aid by the Japan Society for the Promotion of Science.

References

1. D. G. Morris, *Materials Science Foundations 2, Mechanical behavior of nanostructured materials*, Trans. Tech. Publications Ltd, (1998), 1.
2. C. Suryanarayana, *International Materials Reviews*, 40 (1995), 41-64.
3. R. Z. Valiev, R. K. Islamgaliev and I. V. Alexandrov, *Progress in Materials Science*, 45 (2000), 103-189.
4. M. Umemoto, *Mater. Trans.* 44 (2003) in press.
5. J. S. C. Jang and C. C. Koch, *Scr. Metal.* 24 (1990), 1599-1604.
6. H. J. Fecht, E. Hellstern, Z. Fu and W. L. Johnson, *Met. Trans.* 21A (1990), 2333-2337.
7. R. Z. Valiev, Y. V. Ivanisenko, E. F. Rauch and B. Baudelet, *Acta Mater.* 44(1996), 4705-4712.
8. M. Umemoto, B. Haung, K. Tsuchiya and N. Suzuki, *Scr. Mater.* 46 (2002), 383-388.
9. M. Umemoto, Y. Todaka and K. Tsuchiya, *Mater. Trans.* 44 (2003), 1494-1502.
10. P. Heilmann, W. A. T. Clark and D. A. Rigney, *Acta Metall* 31 (1983), 1293-1305.
11. N. R. Tao, M. L. Sui, J. Lu and K. Lu, *NanoStructured Mater.* 11 (1999), 433-440.
12. I. Altenberger, B. Scholtes, U. Martin and H. Oettel, *Mater. Sci. Eng. A* 264 (1999), 1-16.
13. J. Yin, M. Umemoto, Z. G. Liu and K. Tsuchiya, *ISIJ Int.* 41 (2001), 1391-1396.
14. G. Langford and M. Cohen, *Trans. of the ASM* 62 (1969), 623-638.
15. H. Tashiro, *Doctor thesis at Tohoku Univ.* (1992).
16. R. Z. Valiev, Y. V. Ivanisenko, E. F. Rauch and B. Baudelet, *Acta Mater.* 44 (1996), 4705-4712.
17. R. Kaibyshev, I. Kazakulov, T. Sakai and A. Belyakov, *Proc. of Int. Symp. on Ultrafine Grained Steels* (The Iron and Steel Inst. of Japan, 2001), 152-155.
18. M. Umemoto, X. J. Hao, T. Yasuda and K. Tsuchiya, *Materials Transaction*, 43 (2002), 2536-2542.
19. D. A. Hughes and N. Hansen, *Acta Mater.* 48 (2000), 2985.